A thermodynamic model for calculating the operating process in the cylinder of a spark-ignition engine with internal mixture formation and stratified air-fuel charge based on the volume balance method was developed. The model takes into account the change in the working fluid volume during the piston movement in the cylinder.

The equation of volume balance of internal mixture formation processes during direct fuel injection into the engine cylinder was compiled. The equation takes into account the adiabatic change in the volume of the stratified air-fuel charge, consisting of fuel-air mixture volume and air volume. From the heat balance equation, the change in the fuel-air mixture volume during gasoline evaporation in the fuel stream and from the surface of the fuel film due to external heat transfer was determined.

Basic equations of combustion-expansion processes of the stratified air-fuel charge were derived, taking into account three zones corresponding to combustion products, fuel-air mixture and air volumes. The equation takes into account the change in the working fluid volume due to heat transfer and heat exchange between the zones and the walls of the above-piston volume. Dependences for determining the temperature in the three considered zones and pressure in the cylinder were obtained.

Graphs of changes in the volumes of the combustion products, fuel-air mixture and air zones with the change of the above-piston volume in partial load modes (n=3,000 rpm) were plotted. With increasing load from bmep=0.144 MPa to bmep=0.322 MPa, at the moment of fuel ignition, the volume of the fuel-air mixture increases from 70 % to 92 % of the above-piston volume. At the same time, the air volume decreases from 30 % to 8 %.

Analysis of theoretical and experimental indicator diagrams showed that discrepancies in the maximum combustion pressure do not exceed 5 %

Keywords: three-zone combustion model, engine operating process, stratified air-fuel charge

UDC 621.43.01
DOI: 10.15587/1729-4061.2021.228812

DEVELOPMENT OF A THREE-ZONE COMBUSTION MODEL FOR STRATIFIED-CHARGE SPARK-IGNITION ENGINE

Volodymyr Korohodskyi
Doctor of Technical Sciences, Associate Professor*
E-mail: korohodskyi@khadi.kharkov.ua
Andrii Rogovyi
Doctor of Technical Sciences, Associate Professor
Department of Theoretical Mechanics and Hydraulics**
Oleksandr Voronkov
Doctor of Technical Sciences, Professor*
Andrii Polivyanchuk
Doctor of Technical Sciences, Professor
Department of Urban Environmental Engineering
O. M. Beketov National University of Urban Economy in Kharkiv
Marshala Bazhanova str., 17, Kharkiv, Ukraine, 61002
Pavlo Gakal
Doctor of Technical Sciences, Associate Professor***
Oleksii Lysytsia
PhD, Associate Professor***
Igor Khudiakov
Senior Lecturer
Department of Operation of Ship Power Plants
Kherson State Maritime Academy
Ushakova ave., 20, Kherson, Ukraine, 73000
Tamara Makarova
PhD
Department of Automobiles and Transport Management
Vinnytsia National Technical University
Khmelnytsky highway, 95, Vinnytsya, Ukraine, 21021
Mariia Hnyp
PhD
Department of Technological Transport
Ivano-Frankivsk National Technical University of Oil and Gas
Karpatska str., 15, Ivano-Frankivsk, Ukraine, 76019
Yevhen Haiek
PhD
Department of Optimization of Technological Systems named after T. Yevsiukov
Kharkiv Petro Vasylenko National Technical University of Agriculture
Alchevskykh str., 44, Kharkiv, Ukraine, 61002
*Department of Internal Combustion Engines**
**Kharkiv National Automobile and Highway University
Yaroslava Mudroho str., 25, Kharkiv, Ukraine, 61002
***Department of Aerospace Thermal Engineering
National Aerospace University «Kharkiv Aviation Institute»
Chkalova str., 17, Kharkiv, Ukraine, 61070

Received date 11.03.2021
Accepted date 16.04.2021
Published date 22.04.2021

How to Cite: *Korohodskyi, V., Rogovyi, A., Voronkov, O., Polivyanchuk, A., Gakal, P., Lysytsia, O., Khudiakov, I., Makarova, T., Hnyp, M., Haiek, Y. (2021). Development of a three-zone combustion model for stratified-charge spark-ignition engine. Eastern-European Journal of Enterprise Technologies, 2 (5 (110)), 46–57. doi: https://doi.org/10.15587/1729-4061.2021.228812*

1. Introduction

Despite the global record decline in CO_2 emissions [1], which characterizes mainly the amount of fuel burned, the share of renewable energy consumption is increasing due to lower demand in the global energy sector.

Therefore, current requirements for fuel consumption, including alternative, and toxic emissions into the atmosphere

pose a complex problem of efficiency of internal combustion engines (ICE) [2].

Fuel consumption and toxic exhaust gas (EG) emissions of road transport can be reduced using hybrid drives [3] based on ICE, alternative to them or with electric traction.

To this end, studies have been carried out to improve the reliability of traction induction motors of electric vehicles [4]. Using mathematical modeling of operating processes of pneumatic motors, the possibility of installing them in low-tonnage vehicles as the main or auxiliary power generating system was estimated [5].

A modern solution to the problem of reducing harmful EG emissions of land and water transport [6] is the conversion of existing ICE to gas [7], alcohol [8] and alternative fuels [9].

An effective way to increase the technical and economic [10] and environmental performance [11] of spark-ignition (SI) engines is organizing internal mixture formation with direct injection (DI) and ensuring combustion of stratified fuel-air charge (SFAC) [12].

It is promising to use two-stroke DI SI engines having higher specific torque and effective power at partial loads compared to four-stroke ICE. At the same time, two-stroke SI engines have high specific weight and volume [13], which helps to expand their scope and reduce cost.

In the direction of converting ICE to renewable fuels, studies were carried out on using gasoline-ethanol mixtures on a 1D 8.7/8.2 two-stroke DI SI engine [14].

Rather high technical-economic and environmental performance of the 1D 8.7/8.2 s DI SI engine when operating on gasoline was obtained [15]. An increase in engine parameters was due to effective interaction of gas exchange [16], mixture formation [17] and stratified fuel-air charge (FAC) combustion processes [18].

To further meet the current standardized requirements for harmful EG emissions [1] and reduce the consumption of various fuels, it is advisable to carry out scientific research using mathematical modeling of ICE operation.

The results of modeling will allow evaluating and predicting the impact of the peculiarities of internal mixture formation and SFAC combustion processes, identifying the main factors affecting engine performance. At the same time, the results will reduce the time and cost of experimental research.

Therefore, the development and refinement of mathematical models of ICE operation are relevant.

2. Literature review and problem statement

The thermodynamic method for calculating the ICE operating process is widely used in practice. One-zone, two-zone and multi-zone models have become widespread.

The work [19] uses the thermodynamic method, in particular, to calculate an ideal operating cycle of the SI engine according to the one-zone model, which does not take into account heat transfer during internal mixture formation.

The one-zone multistage model [20] for calculating the two-stroke engine specifies stages of scavenging processes, but does not take into account joint processes of mixture formation with DI in the cylinder and open valves.

In [21], using the one-zone thermodynamic model for calculating the operating process of biogas SI engines, the Vibe combustion formula was specified, while it would also be desirable to specify a heat transfer formula.

The zero-dimensional diagnostic model [22] allows real-time calculation of the combustion process, determining the gas temperature in the cylinders in stationary and transient modes, but the model can only be used for diesel engines.

One-zone models allow conducting the thermodynamic analysis of the ICE cycle [23], determining specific fuel consumption, torque, power, thermal efficiency [24] and power balance [25]. But there are still unresolved issues related to modeling the processes in the cylinder in the mixture formation and combustion zones, which limits the completeness of the description and understanding of these processes.

Intra-cylinder processes are considered in more detail in two-zone models [26–30], which take into account two zones during the combustion process: the zone of combustion products (CP) and the zone of fuel-air mixture (FAM).

At the same time, two-zone models present the following assumptions:

– in the above-piston volume, during the combustion process, the CP zone is separated from the unburned FAM zone by the flame front surface;

– at each timepoint, the composition of the FAM zone is homogeneous, the composition of the CP zone is assumed equilibrium;

– the speed of the flame front is much less than the speed of sound, so the pressure in the above-piston volume is assumed identical, and temperatures in the FAM and CP zones are different.

In the two-zone model [26], the above-piston volume during combustion is divided by the flame front into the unburned FAM zone and the CP zone. The zones under consideration are characterized by the following values: temperature T, volume V, number of moles of zone components n_i and air-fuel ratio λ in the FAM zone.

The model takes into account heat losses to the walls of the above-piston volume due to radiation and convection. The surface areas of the flame front and both zones are unknown. The model considers the air mass passed through the flame front from the FAM zone to the CP zone and the excess air mass not participating in combustion ($\lambda>1$). However, the model does not include heat release from the flame front in the FAM zone.

In the two-zone thermodynamic model [27], the total volume occupied by the working fluid in the above-piston volume of the engine is divided during combustion into two zones – unburned FAM zone and CP zone. Each zone has the following parameters: instantaneous value of volume V and mass m, temperature T, specific enthalpy h, specific internal energy u and gas constant R.

The model considers the heat transfer from each zone to the walls of the above-piston volume and the heat transfer between the burned and unburned zones, which brings the mathematical description closer to actual processes. However, the model does not take into account the possible SFAC, where, in addition to the FAM and CP zones, there is the air zone that does not participate in the combustion process.

In [28], the two-zone model characterizes the FAM and CP zones by the following parameters: total pressure p, temperature T, volume V, and mass change dm of the working fluid in each zone. The process of heat release in the CP zone is taken into account. To simulate the combustion process, gas equations for the zones, mass and energy balance are used. The model takes into account heat and mass transfer between the FAM and CP zones during combustion. In the combustion reaction zone, the local air-fuel ratio λ_{loc} is

calculated taking into account the EG content. The mathematical model considers the heat transfer to the walls of the above-piston volume in each zone. The disadvantage of the model is that it does not take into account the air zone when organizing SFAC.

In the two-zone model [29], the above-piston volume during combustion is divided by the propagating flame front into two zones: FAM and CP. Each zone has the temperature T and the same pressure p throughout the above-piston volume. Heat transfer between the zones is taken into account by the radiation component.

In the model, during combustion, the mass flow rate of the FAM depends on the area of the flame front, which propagates from the ignition source in the form of a sphere bounded by the walls of the combustion chamber, cylinder and the surface of the moving piston head. The of the flame front surface is approximated in the form of a sphere surface, the geometry of the combustion chamber and the location of the spark plug electrodes are taken into account. The volume of the CP zone is calculated as a function depending on the radius of the propagating flame front.

The new two-zone thermodynamic model for SI engines estimates variable parameters of the CP and FAM zones with high accuracy. The simplified structure of the model, consisting of two ordinary differential equations, describes an idealized thermodynamic process in the unburned zone, which allows increasing computing speed to the level of one-zone model [30].

Two-zone models do not allow determining local parameters of the working fluid in the CP and FAM zones, which reduces the reliability of determining the rate of nitrogen oxide formation.

The use of the multi-zone model, considering the division of the above-piston volume into 13 zones during combustion [31], makes it possible to positively influence the accuracy of modeling temperatures in the zones.

In [32], the three-zone model is presented, in which, in addition to the CP and FAM zones, a combustion zone near the walls is introduced, where the temperature is lower than in the main reaction zone due to heat loss into the walls. Using several zones allows taking into account temperature and concentration gradients of the FAM in the flame front.

The development of a multi-zone combustion model is given in [33], which presents detailed chemical kinetics based on a thermodynamic model for calculating CP formation in a natural gas engine.

In [34], a multi-zone model is presented that can predict the heat flow to the walls and laminar flame quenching distance in the FAM of synthesis gas and air. The use of the multi-zone combustion model [35] allows estimating the effect of the initial turbulization rate and hydrogen volume fraction in synthesis gas in the FAM zones on the outward propagation velocity of turbulent flame.

Using the method of thermodynamic modeling of multi-zone combustion [36] of lean methane-air mixtures, taking into account experimental results, made it possible to prove higher efficiency of laser ignition compared to SI.

In [37], a multi-zone phenomenological model of flame combustion was used, which allows predicting the characteristics and harmful emissions of SI engines. The model takes into account flame combustion turbulence, flame geometry interaction with the walls, heat transfer from the gas to the walls, CO and NO emissions from combustion zones and hydrocarbon emissions from relatively cold zones.

In the considered single-zone, two-zone and multi-zone models, the possibility of formation of an air zone when organizing SFAC in the above-piston volume is omitted. At the same time, the peculiarities of internal mixture formation and SFAC combustion processes are not fully taken into account, which limits the determination of local parameters of the working fluid simultaneously in the CP, FAM and air zones. Therefore, developing a three-zone model considering SFAC in the above-piston volume during mixture formation (FAM and air zones) and combustion (CP, FAM and air zones) of zones by layers seems relevant.

3. The aim and objectives of the study

The aim of the work is to develop a three-zone thermodynamic model based on the volume balance method for calculating the operating processes of the SFAC SI engine.

To achieve the aim, the following objectives were set:

– to draw up a differential equation for internal mixture formation, including compression stroke heat balance, taking into account the change in heat due to heat transfer to the adjoining walls and gasoline evaporation in the fuel stream and from the fuel film;

– to derive basic equations of the three-zone model of the SFAC combustion-expansion processes, differential equation taking into account three zones corresponding to the CP, FAM and air volumes, equations for the heat flow change in the zones;

– to derive dependencies for determining the working fluid parameters: pressure in the above-piston volume during combustion and temperatures in the zones (CP, FAM and air), taking into account heat transfer;

– to build graphs of changes in the volumes of the FAM, CP and air zones with the change of the above-piston volume in partial load modes according to the load characteristic;

– to compare the results of theoretical and experimental studies using indicator diagrams and determine the average temperature in the above-piston volume and zones (CP, FAM and air) using a three-zone combustion model.

4. Materials and methods for studying operating processes of the DI SI engine

The theoretical and experimental studies are based on the fundamental provisions of the ICE theory, basic laws of thermodynamics and heat transfer using mathematical and physical modeling methods, methods of parametric identification of mathematical models.

Theoretical studies of engine operation are based on the thermodynamic method of volume balance.

The general differential equation takes into account the change in the above-piston volume over time ($d\tau$) with the piston movement in the cylinder and the change in the working fluid volume during ICE operation (Fig. 1).

The differential equation is based on the volume balance [38] and gas exchange equations [39].

$$dV_{apv} = dV_{ad} + dV_s + dV_f + \\ + dV_{leakage} + dV_{losses} + dV_{mol} + dV_Q, \quad (1)$$

where dV_{apv} – change in the above-piston volume during piston movement (m^3), dV_Q – change in the volume of the working fluid in the above-piston volume due to heat trans-

fer (m^3), $dV_{ad}=-(V_{apv}/k\cdot p)dp$ – adiabatic volume change with pressure change p, obtained from the adiabatic equation $p\cdot v^{\gamma}=$constant ($\gamma=C_p/C_v$ – the ratio of specific heats for the gas, where C_p is the specific heat at constant pressure and C_v is the specific heat at constant volume) (m^3), dV_s – change in the volume of fresh charge (air or FAM) with parameters (p_S and T_S) in front of intake valves, which entered the above-piston volume (m^3), dV_{CP+air} – change in the volume of the CP and a part of the air charge that did not participate in combustion with parameters (p_T and T_T) after exhaust valves, released from the above-piston volume (m^3), $dV_{leakage}$ – change in the volume of the working fluid (air and/or FAM, as well as CP), released from the above-piston volume during its leakage with overlapped (intake and exhaust) valves (m^3), dV_{losses} – change in the volume of the working fluid released from the above-piston volume due to losses through clearance between piston rings and cylinder walls (m^3), dV_{mol} – change in the volume of the working fluid in the above-piston volume due to the change in the number of moles in the FAM and during combustion processes (m^3).

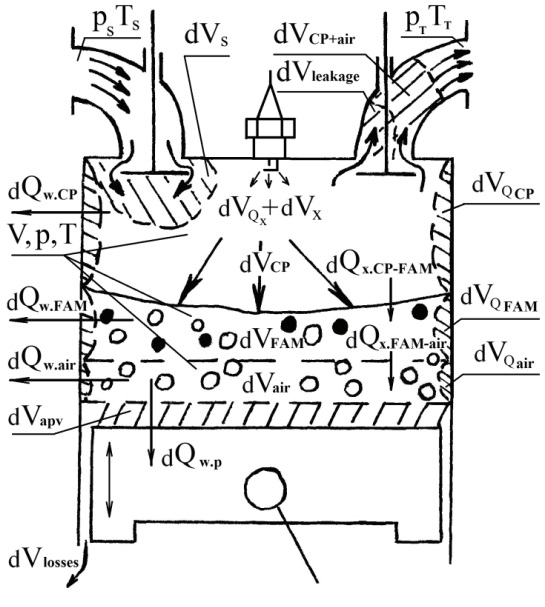

Fig. 1. Design diagram of SFAC SI engine operation

The developed three-zone thermodynamic model for calculating the operating processes of the SFAC SI engine was implemented in the Matlab programming environment.

The results of modeling, in particular, the indicator diagram showing the change in the gas pressure in the engine cylinder by the crank angle, were compared with the experimental indicator diagrams.

To study the actual processes in the above-piston volume of the engine, the experimental-statistical method of signal processing by measuring equipment based on the least-squares method was used.

Experimental studies of ICE operation were carried out on the Schenk hydraulic brake motor bench. The bench is equipped with instruments that allow researching engine operation in accordance with ISO 3046-3:2006.

To record the indicator diagrams, a measuring system based on the E14-140 analog-to-digital converter (ADC) manufactured by L-Card (L-783 motherboard). was used. The pressure in the engine cylinder was measured using the 8QP505CS piezometric pressure sensor manufactured by AVL and PowerGraph software (Russia) in order to process signals from sensors. Processing of indicator diagrams to determine combustion pattern (m), combustion duration (φ_z), fuel burnup characteristic was carried out according to the Vibe method using the written program in Mathlab.

The EG toxicity was monitored with the CT 300.02 gas analyzer. Gas analysis by the device for SI engines corresponds to the 1st accuracy class.

The experiment and estimation of measurement errors were carried out on the basis of the recommendations set forth in [40, 41].

The developed three-zone model based on the volume balance method is used to calculate the operating process [42] of the 1D 8.7/8.2 s two-stroke DI SI engine, the parameters are given in Table 1.

Table 1

Parameters of the 1D 8.7/8.2 s two-stroke DI SI engine

Parameters	Unit of measurement	Value
Maximum power (at n=4,500 rpm)	kW	15
Diameter	mm	82
Stroke	mm	87
Compression ratio (geometric/real)	–	16.3/11.3
Fuel	–	gasoline A-80
Number of cylinders	–	1
Ignition dwell angle	CAD BTDC	10
Fuel injection point at the maximum fuel delivery per stroke	CAD ATDC	224

The engine is air-cooled and crankcase-scavenged. DI makes it possible to organize stratified lean fuel-air charge [43]. Experimental indicator diagrams were obtained in load characteristic modes at n=3,000 rpm.

5. Results of studies of the operating process of the stratified fuel-air charge SI engine

5. 1. Differential equation of the volume balance of internal mixture formation processes

The equation describes the course of internal mixture formation processes of the SFAC DI SI engine at the compression stroke (Fig. 1) with closed valves (general view):

$$dV_{apv}=dV_{ad}+dV_s+dV_{CP+air}+dV_{leakage}+dV_{losses}+dV_Q. \quad (2)$$

The left side of the equation (dV_{apv}) corresponds to the change in the above-piston volume during the piston movement. The right side of the equation considers the sum of changes in the working fluid volumes.

Adiabatic change in the volume of the stratified FAC, consisting of FAM volume and air volume with the distribution of CP residues over the considered volumes, m^3:

$$dV_{ad}=-\frac{dp}{p}\left(\frac{V_{FAM}}{\gamma_{FAM}}+\frac{V_{air}}{\gamma_{air}}\right), \quad (3)$$

where p, dp – pressure and pressure change in the above-piston volume V_{apv}, respectively (Pa), V_{FAM} – volume of FAM with a part of CP (m^3), V_{air} – air volume with a part of CP (m^3),

γ_{FAM} – adiabatic index in the volume of FAM with a part of CP, γ_{air} – adiabatic index in the volume of air with a part of CP.

The change in the volume of the working fluid in the above-piston volume due to external heat transfer, m^3:

$$dV_Q = dV_{Q_w} + dV_{Q_{evaporation}}, \quad (4)$$

where $dV_{Q_{evaporation}}$ – change in the volume of FAM with a part of CP (V_{FA}) due to liquid fuel evaporation (m^3), dV_{Qw} – change in the volume of the working fluid due to heat exchange with the walls of the above-piston volume (m^3):

$$dV_{Q_w} = dV_{FAM} + dV_{air}, \quad (5)$$

where dV_{FAM} – change in the elementary volume of FAM with a part of CP (m^3), dV_{air} – change in the elementary volume of air with a part of CP (m^3).

The change in the volume of FAM in the above-piston volume due to physical processes during liquid fuel evaporation (m^3) [38]:

$$dV_M = dV_{physic\ process\ of\ evaporation\ \ FA} = \\ = \frac{V_{FAM}}{M} dM_{physic\ process\ of\ evaporation}, \quad (6)$$

where M – number of FAM moles (kmol), $dM_{physic\ process\ of\ evaporation}$ – change in the number of molecules during physical processes of liquid fuel evaporation (kmol):

$$dM_{physic\ process\ of\ evaporation} = \\ = A \frac{p_{saturated\ steam} - p_{partial\ vapor\ pressure}}{p_{apv}}, \quad (7)$$

where p_{apv} – pressure in the above-piston volume (Pa), $p_{saturated\ steam}$ – saturated steam pressure of evaporating liquid fuel (Pa), $p_{partial\ vapor\ pressure}$ – partial vapor pressure at the evaporation temperature of liquid fuel (Pa), A – coefficient depending on evaporation surface, gas and liquid relative flow rate, etc.

The change in the FAM volume, composition and air volume over time ($d\tau$) is preferably determined by analytical studies of three-dimensional gas dynamics and directly by experiment.

With insignificant losses of the working medium (dV_{losses}) from the above-piston volume through the clearance between piston rings and cylinder walls, these values are not taken into account in the calculations.

Heat balance at the compression stroke.

$$dQ = dQ_w - \begin{pmatrix} dQ_{evaporation\ of\ gasoline\ in\ a\ fuel\ jet} + \\ + dQ_{evaporation\ from\ the\ surface\ of\ the\ fuel\ film} \end{pmatrix}, \quad (8)$$

where dQ_w – change in the amount of heat due to heat transfer between the working fluid in the above-piston volume and the adjoining walls over a period ($d\tau$) (J),

$$dQ_w = \alpha_w \cdot F_w \left(T_w - T_{working\ fluid}\right) d\tau, \quad (9)$$

where F_w – current surface area of the walls of the above-piston volume (m^2), T_W – average wall temperature over the surface of the above-piston volume F_w (K), $T_{working\ fluid}$ – current temperature of the working fluid (K), α_w – heat transfer coefficient between the gas and the walls of the above-piston volume ($W/m^2 \cdot K$).

For the 1D 8.7/8.2 two-stroke, crankcase-scavenged, air-cooled DI SI engine, the Woschni heat transfer formula was corrected [44] for the combustion-expansion section for the three-zone combustion model, $W/m^2 \cdot K$ [45]:

$$\alpha_w = 100 D^{-0.2} \left(p_{apv} \cdot 10^{-5}\right)^{0.75} T^{-0.55} \times \\ \times \left[C_1 \cdot C_m + C_2 \frac{V_{apv} \cdot T_a}{p_a \cdot V_a} \left(p_{apv} - p_0\right) \right]^{0.75}, \quad (10)$$

where D – cylinder diameter (m), p_{apv}, p_0 – pressure in the above-piston volume with the engine running and cranking, respectively (MPa), p_a, V_a, T_a – pressure (MPa), volume (m^3) and temperature (K) in the above-piston volume at the time of closing valves, respectively, V_{apv}, V_φ, V_c – above-piston volume, current above-piston volume, combustion chamber volume, respectively (m^3), $C_1 = 2.28 + 0.308 \cdot (C_t / C_m)$ – constant in the compression-combustion-expansion section (C_t and C_m – tangential speed of the working fluid near the walls of the above-piston volume and average piston speed, respectively (m/s), $C_2 = 2.24 \cdot 10^{-4}$, (K^{-1}) – corrected constant taking into account the organization of the process of volume-film mixing and combustion of the stratified lean FAC [46].

The change in the amount of heat over a period ($d\tau$) during gasoline evaporation in the fuel jet, for example, based on the wake theory, according to the method proposed in [47]:

$$dQ_{evaporation\ of\ gasoline\ in\ a\ fuel\ jet} = \\ = \alpha_0 \cdot F_D \left(T_c - T_s\right) d\tau = \alpha_0 \cdot \pi \cdot D^2 \left(T_c - T_s\right) d\tau, \quad (11)$$

where α_0 – heat transfer coefficient from gas to droplet ($W/m^2 \cdot K$), T_c – average temperature in the above-piston volume (K), T_s – saturation temperature (K), D – average droplet diameter in the front of the fuel jet (m).

The change in the amount of heat during the evaporation of the fuel film located on the surfaces of the combustion chamber over a period ($d\tau$) is determined from the condition for the balance of heat supplied to the liquid film and spent on its evaporation. The process of fuel film evaporation can be calculated, for example, by the method, J [48]:

$$dQ_{evaporation\ from\ the\ surface\ of\ the\ fuel\ film} = \\ = \begin{bmatrix} \alpha_{air} \left(t_{environment} - t_{evaporation}\right) + \\ + \alpha_{fuel} \left(t_{fuel} - t_{evaporation}\right) \end{bmatrix} d\tau = \\ = \beta_{evaporation\ coefficient} \cdot p_{above\ the\ surface\ of\ the\ fuel\ film} \cdot \Delta i, \quad (12)$$

where α_{air}, α_{fuel} – heat transfer coefficients of air and fuel, respectively ($W/m^2 \cdot K$), $\beta_{evaporation}$ – evaporation coefficient related to the difference in partial vapor pressures above the surface of the fuel film $p_{above\ the\ surface\ of\ the\ fuel\ film}$ and in the environment, Δi – increase in fuel enthalpy (J), $t_{environment}$, t_{fuel}, $t_{evaporation}$ – temperature: ambient air, fuel film surface from the side of the heated surface and evaporation (°C), respectively.

Pressure change equation for the single-zone model for calculating the engine operating process.

To calculate the operating process at the compression stroke, we take the one-zone model as a basis and consider the adiabatic index and temperature in the above-piston volume as average [39, 45, 49].

Taking into account the processes of fuel evaporation during internal mixture formation at the compression stroke, it is proposed to calculate the pressure change in the above-piston volume by the formula, Pa:

$$dp = p \cdot \frac{k}{V_{apv}} \cdot \left(\pm \frac{k-1}{k} \cdot \frac{\pm dQ_w - dQ_{evaporation}}{p} - dV_{apv} \right), \quad (13)$$

where dQ_w is the amount of heat supplied or removed from the working fluid to adjacent walls, J;

$$dQ_{evaporation} = dQ_{evaporation\ of\ gasoline\ in\ a\ fuel\ jet} + \\ + dQ_{evaporation\ from\ the\ surface\ of\ the\ fuel\ film}$$

is the amount of heat spent for fuel evaporation in the fuel jet $dQ_{evaporation\ of\ gasoline\ in\ a\ fuel\ jet}$ and from the surface of the fuel film $dQ_{evaporation\ from\ the\ surface\ of\ the\ fuel\ film}$, (J).

Temperature change equation for the single-zone model for calculating the engine operating process.

Assuming that the temperature at the compression stroke in the FAM and air volumes is the same, and has an average value ($T_{average}$), if we take $dp=(T_{average}/V_{apv})\cdot dV_{apv}$, after transformations, the temperature change equation, (K), takes the following form:

$$dT_{average} = \frac{T_{average}}{V_{apv}} \left(\begin{array}{l} \frac{k-1}{k} \cdot \frac{V_{apv}}{p} dp + \\ + \frac{k-1}{k} \cdot \frac{\pm dQ_w - dQ_{evaporation}}{p} \end{array} \right). \quad (14)$$

5. 2. Three-zone combustion model for the stratified fuel-air charge SI engine

In partial load modes, when organizing SFAC, during combustion, three zones or three volumes are formed in the above-piston volume (dV_{apv}). The CP volume (V_{CP}) in the combustion zone, FAM volume with a part of CP (V_{FAM}) and air volume (V_{air}) with a part of CP, remained from the previous cycle.

The CP and FAM zones are separated by the flame front, the FAM and air zones are conditionally separated from each other (Fig. 1) and do not mix during combustion.

The volumes of the CP, FAM and air zones are related by the ratio, respectively, during the combustion-expansion processes:

$$V_{CP} + V_{FAM} + V_{air} = V_{apv}. \quad (15)$$

With full flame engulfment of the FAM (completion of combustion processes) and during expansion:

$$V_{CP} + V_{air} = V_{apv}. \quad (16)$$

Ratios of volumes in the zones:

$$\upsilon_{CP} = \frac{V_{CP}}{V_{apv}} \text{ – for the CP zone;} \quad (17)$$

$$\upsilon_{FAM} = \frac{V_{FAM}}{V_{apv}} \text{ – for the FAM zone;} \quad (18)$$

$$\upsilon_{air} = \frac{V_{air}}{V_{apv}} \text{ – for the air zone.} \quad (19)$$

Taking into account the piston movement and the combustion process in the cylinder, we have volume changes in the zones:

$$dV_{CP} = -dV_{FAM} \text{ – zone of CP volume change;} \quad (20)$$

$$dV_{FAM} = V_{FAM} dx \text{ – zone of FAM volume change;} \quad (21)$$

$$dV_{air} = \upsilon_{air} dV_{apv} \text{ – zone of air volume change.} \quad (22)$$

The differential equation of the volume balance of combustion-expansion processes taking into account three zones in the V_{CP}, V_{FAM} and V_{air} volumes (general view):

$$dV_{apv} = dV_{ad} + dV_x + dV_Q, \quad (23)$$

where

$$d_{ad}V = -\frac{dp}{p} \left(\frac{V_{CP}}{\gamma_{CP}} + \frac{V_{FAM}}{\gamma_{FAM}} + \frac{V_{air}}{\gamma_{air}} \right), \quad (24)$$

$$d_x V = (\beta - 1) V_{FAM} dx, \quad (25)$$

where $d_x V$ is the change in the working fluid volume due to the change in the number of molecules during chemical combustion processes, m^3; β is the molecular change coefficient; x is the fuel share in the FAM volume (V_{FAM}) reacted during combustion for the calculated time interval ($d\tau$).

The change in the volume of the working fluid in the above-piston volume due to heat transfer and heat exchange between the zones and the walls of the above-piston volume, m^3 (Fig. 1) (general):

$$dV_Q = \frac{\gamma - 1}{\gamma} \cdot \frac{dQ_x \pm dQ_w}{p_{apv}}. \quad (26)$$

The change in the amount of released heat dQ_x during fuel combustion for the calculated period ($d\tau$) is determined by the dependence:

$$dQ_x = Q_{LHV} \cdot \Delta m_f \cdot dx, \quad (27)$$

where Δm_f is the mass fuel delivery per stroke into the above-piston volume, *kg*, Q_{LHV} is the lowest heat of fuel combustion, kJ/kg; x is the share of fuel burned.

It is assumed that the amount of fuel burned is 99.9 %. To determine the fuel burnup characteristic x by the crank angle φ, the Vibe dependence is used [50]:

$$x = 1 - \exp\left[-6.908 \left(\frac{\varphi - \varphi_c}{\varphi_z - \varphi_c} \right)^{m+1} \right], \quad (28)$$

where φ_c, φ_z are CAD angles of the beginning and end of combustion, respectively; φ is the conditional duration of the combustion process; m is the combustion pattern.

The values of φ_c, $d\varphi_z$ and m are determined by processing experimental indicator diagrams [46].

The change in the heat flux for the CP zone with the temperature T_{CP} is taken into account by the heat transfer to the adjoining walls ($dQ_{w.CP}$) with temperature T_W and to the FAM zone ($dQ_{x.CP\text{-}FAM}$) with temperature T_{FAM}. Heat transfer occurs through the corresponding surface areas ($F_{w.CP}$ and $F_{w.CP\text{-}FAM}$) taking into account the radiation heat flux (dQ_R). The heat flux dQ_R acts over the entire surface area (F_{CP}) surrounding the CP zone in the form of a heat balance (29) and over time ($d\tau$) (30):

$$dQ_{CP} = dQ_{w.CP} + dQ_{x.CP\text{-}FAM} + dQ_R, \quad (29)$$

$$\frac{dQ_{CP}}{dt} = a_{CP} (T_{CP} - T_w) F_{w.CP} + \\ + k_{CP\text{-}FAM} (T_{CP} - T_{FAM}) F_{w.CP\text{-}FAM} + dQ_R, \quad (30)$$

where α_{CP} is the heat transfer coefficient for the CP zone, adjoining the walls of the above-piston volume, W/m^2 K;

$k_{CP\text{-}FAM}$ is the heat transfer coefficient between the CP and FAM zones; dQ_R is the radiation heat transfer.

Convective heat transfer, referred to the zones separation area, is considered as heat transfer between the zones through the flame front surface and FAM and air separation surface (zone interfaces).

Assuming that the thickness of the front line is $\Delta \to 0$, the heat transfer coefficient for the CP and FAM zones is the reduced heat transfer coefficient [27]:

$$k_{CP-FAM} = \frac{\alpha_{CP} \cdot \alpha_{FAM}}{\alpha_{CP} + \alpha_{FAM}}, \quad (31)$$

where α_{CP}, α_{FAM} are the heat transfer coefficients for the CP and FAM zones, respectively [51].

For the area of separation between the CP and FAM zones:

$$dQ_{x.CP-FAM} = k_{CP-FAM}\left(T_{CP} - T_{FAM}\right)F_{w.FAM-CP}d\tau, \quad (32)$$

where $k_{CP\text{-}FA}$ is the heat transfer coefficient of the CP and FAM zones; $F_{w.FAM\text{-}CP}$ is the area of separation of the FAM and CP zones; T_{CP} is the temperature of the CP zone; T_{FAM} is the temperature of the FAM zone.

The change in the heat flux for the FAM zone is taken into account by heat transfer from the CP zone ($dQ_{x.CP\text{-}FAM}$) to the adjoining walls ($dQ_{w.FAM}$) and to the air zone ($dQ_{x.FAM\text{-}air}$). The change in the heat flux is presented as heat balance (33) and over time ($d\tau$) (34):

$$dQ_{FAM} = dQ_{w.FAM} + dQ_{x.CP-FAM} + dQ_{x.FAM-air}, \quad (33)$$

$$\frac{dQ_{FAM}}{d\tau} = \alpha_{FAM}\left(T_{FAM} - T_w\right)F_{w.FAM} + k_{CP-FAM}\left(T_{CP} - T_{FAM}\right)F_{w.CP-FAM} + k_{FAM-air}\left(T_{FAM} - T_{air}\right)F_{w.FAM-air}. \quad (34)$$

The coefficients of heat transfer (k) and heat exchange (α) between the zones (CP and FAM) and the adjoining walls of the above-piston volume are taken by analogy with the CP zone.

The change in the heat flux for the air zone with temperature T_{air} is taken into account by heat transfer ($dQ_{w.air}$) to the adjacent cylinder walls with temperature T_w and in the piston head ($dQ_{w.p}$) with temperature T_p. During the combustion of the FAM zone, heat transfer ($dQ_{x.FAM\text{-}air}$) is carried out from the FAM zone, taking into account the FAM temperature (T_{FAM}). With the complete combustion of the FAM zone, heat transfer ($dQ_{x.CP\text{-}air}$) occurs from the CP zone with temperature (T_{CP}). Heat transfer is carried out through the wall areas ($F_{w.air}$ and $F_{w.p}$) and separation areas between the zones ($F_{w.FAM\text{-}air}$ and $F_{w.CP\text{-}air}$) in the form of heat balance (35) and over time ($d\tau$) (36):

$$dQ_{air} = dQ_{w.air} + dQ_{w.p} + dQ_{x.FAM-air\ or\ CP-air}, \quad (35)$$

$$\frac{dQ_{air}}{d\tau} = \alpha_{air}\left(T_{air} - T_w\right)F_{w.air} + \alpha_{air}\left(T_{air} - T_p\right)\times F_{w.p} + k_{FAM-air\ or\ CP-air}\left(T_{FAM\ or\ CP} - T_{air}\right)\times F_{w.FAM-air\ or\ CP-air}, \quad (36)$$

where $T_{FAM\ or\ CP}$ is the temperature of the working fluid (FAM or CP) in the corresponding time interval (K).

The coefficients of heat transfer and heat exchange between the air and FAM or CP zones are taken for the corresponding time, and with the adjacent cylinder walls and piston head, they are taken into account by analogy with the CP zone. In this case, the contact area of the CP zone with the walls $F_{w.CP}$ is assumed proportional to the corresponding specific volume υ_{CP}:

$$F_{w.CP} = F_w(\tau)\cdot\upsilon_{CP}, \quad (37)$$

where $F_W(\tau)$ is the total instantaneous area of the heat-receiving surface of the above-piston volume.

The contact areas of the FAM $F_{W.FAM}$ and air zones $F_{w.air}$ with the walls of the above-piston volume are determined respectively by analogy with the CP zone.

5. 3. Dependencies for determining working fluid parameters

The pressure change in the above-piston volume during combustion, taking into account the volumes presented in the CP, FAM and air zones:

$$dp = p\frac{k_{CP}\cdot k_{FAM}\cdot k_{air}}{V_{CP}\cdot k_{FAM}\cdot k_{air} + V_{FAM}\cdot k_{CP}\cdot k_{air} + V_{air}\cdot k_{CP}\cdot k_{FAM}}\times \times\left[V_{FAM}\cdot(\beta-1)\cdot dx + \frac{\gamma-1}{\gamma}\cdot\frac{dQ_x - dQ_w}{p} - dV_{apv}\right]. \quad (38)$$

Determination of the gas temperature in the zones of the above-piston volume during the combustion process.

The change of the temperature of the working fluid in the CP zone, taking into account heat transfer at $V_{CP}>0$:

$$dT_{CP} = \frac{1}{V_{CP}\cdot C_{v.CP}}\left[\begin{matrix}\left(dQ_x - dQ_{w.CP}\right)- \\ - C_{v.CP}\cdot T_{CP}\cdot dV_{CP} - p\cdot dV_{CP}\end{matrix}\right], \quad (39)$$

where $C_{v.CP}$ is the heat capacity at constant volume of CP.

The change of the temperature of the working fluid in the FAM zone, taking into account heat transfer:

$$dT_{FAM} = \frac{\gamma_{FAM}-1}{\gamma_{FAM}}\cdot T_{FAM}\cdot\frac{dp}{p} + \frac{T_{FAM}}{V_{FAM}}\cdot\frac{\gamma_{FAM}-1}{\gamma_{FAM}}\cdot\frac{dQ_{FAM}}{p}. \quad (40)$$

The change of the temperature of the working fluid in the air zone, taking into account heat transfer:

$$dT_{air} = \frac{\gamma_{air}-1}{\gamma_{air}}\cdot T_{air}\cdot\frac{dp}{p} + \frac{T_{air}}{V_{air}}\cdot\frac{\gamma_{air}-1}{\gamma_{air}}\cdot\frac{dQ_{air}}{p}. \quad (41)$$

The correctness of the calculations is checked by the simultaneous achievement of $\upsilon_{CP}+\upsilon_{air}=1$, $V_{CP}+V_{air}=V_{apv}$ and $V_{FAM}=0$ at the end of the combustion process.

The three-zone model of the operating process of the SFAC SI engine based on the volume balance method allows determining the parameters of the working fluid in the zones of the above-piston volume, depending on the features of internal mixture formation.

5. 4. Graphs of volumes of the fuel-air mixture, combustion products and air zones with the change of the above-piston volume

Modeling of the operating process is carried out taking into account the three-zone combustion model in partial load modes according to the load characteristic at n=3,000 rpm (Fig. 2).

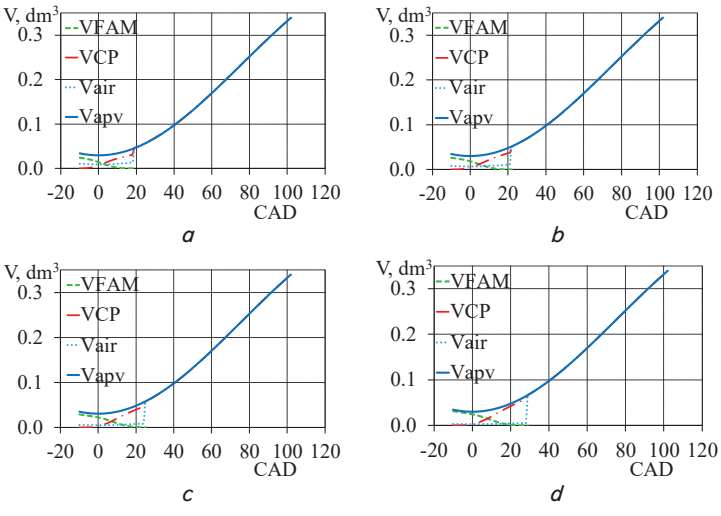

Fig. 2. Changes in the volumes of the FAM (V_{FAM}), CP (V_{CP}) and air (V_{air}) zones with the change of the above-piston volume (V_{apv}) in the modes: *a* – *bmep*=0.144 MPa; *b* – 0.192 MPa; *c* – 0.274 MPa; *d* – 0.322 MPa

When modeling the combustion process according to the three-zone model, at the moment of ignition, in the first approximation, it is assumed that in the maximum load mode, there is no FAM stratification and the FAM volume occupies the entire above-piston volume. The specific FAM volume is $\upsilon_{FAM}=1$. With a decrease in the load and, accordingly, fuel delivery per stroke, the FAM volume in the FAC decreases. In the minimum load mode (*bmep*=0.144 MPa), at the moment of ignition, the specific FAM volume υ_{FAM} is 0.7 (Fig. 2, *a*).

5. 5. Comparison of the results of theoretical and experimental studies by indicator diagrams

Experimental and theoretical indicator diagrams, curves of average temperature changes in the cylinder by the crank angle in the load characteristic modes at *n*=3,000 rpm are presented. Using the three-zone combustion model, the curves of temperature changes in the air, FAM and CP zones were obtained (Fig. 3).

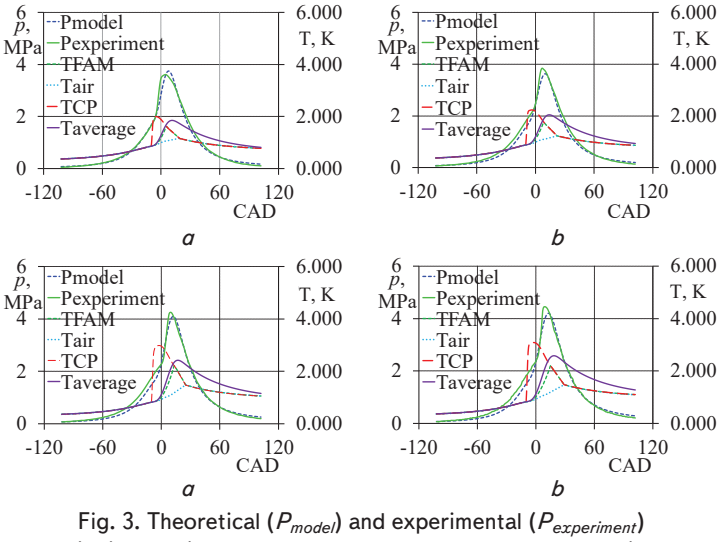

Fig. 3. Theoretical (P_{model}) and experimental ($P_{experiment}$) indicator diagrams, calculated values of temperatures in the cylinder ($T_{average}$), in the CP (T_{CP}), FAM (T_{FAM}) and air (T_{air}) zones in the modes: *a* – *bmep*=0.144 MPa; *b* – 0.192 MPa; *c* – 0.274 MPa; *d* – 0.322 MPa

When using the three-zone combustion model with a change in the FAM volume (V_{FAM}=var), at the moment of ignition, taking into account SFAC peculiarities, the heat transfer formula (10) and the constant C_2 were refined. Correction of the heat transfer formula made it possible to reduce the discrepancy of the p_z values to 5 % in partial load modes (*bmep*=0.322 MPa) between the simulation results and experimental data (Fig. 3).

As a result of the calculation using the three-zone model, the characteristics of temperature changes in the CP, FAM and air zones were determined. After voltage is applied to spark plug electrodes (10 CAD BTDC), the fuel in the FAM zone ignites, forming the CP zone during combustion with an increased temperature before BTDC. With the further course of the combustion process, due to heat transfer from the CP zone, the temperature in the FAM volume zone rises, which subsequently contributes to an increase in the air zone temperature.

The average temperature of the working fluid in the above-piston volume during the combustion process was determined according to the one-zone model (14). The level of average temperatures in the above-piston volume is lower compared to the CP zone determined by the three-zone model and is shifted along the piston movement after ATDC (Fig. 3).

6. Discussion of modeling results compared to experimental data

The analysis of the studies shows that at partial loads when organizing SFAC, it is advisable to use the three-zone model with the change in the FAM volume (V_{FAM}=var) at the moment of ignition (Fig. 2).

As a result of the experiment on the load characteristic at *n*=3,000 rpm, it was found that with an increase in the load and fuel delivery per stroke on the surface of the symmetric hemispherical combustion chamber, the carbon formation spot increases. The area of the carbon formation spot increases in the direction from the spark plug located along the cylinder axis to the peripheral parts of the surface, adjoining the cylinder wall. Thus, based on the experiment and results of 3D modeling [16] of the working fluid motion, an increase in the FAM volume with increasing fuel delivery per stroke from the spark plug electrodes to the cylinder wall was found.

The three-zone combustion model takes into account the change in the volume of the CP, FAM zones and formation of the air zone volume when organizing SFAC in the above-piston volume (15). After fuel ignition (10 CAD BTDC), the FAM volume (21) decreases and the volume of the CP zone (20) increases according to the fuel burnup characteristic (28) and the change in the above-piston volume (23). The volume of the air zone (22) changes in proportion to the above-piston volume and is not mixed with the FAM volume.

With increasing load from *bmep*=0.144 MPa to *bmep*=0.322 MPa, the volume of the FAM zone increases from 70 % (Fig. 2, *a*) of the above-piston volume to 92 % (Fig. 2, *d*). An increase in the FAM zone volume is associated with an increase in the fuel delivery per stroke of DI. At the same operating

conditions of the engine, at the moment of ignition, the volume of the air zone decreases from 30 % to 8 % of the above-piston volume. The volume fraction of the CP zone of the FAM zone volume at the piston position in TDC with increasing load changes from 48 % (Fig. 2, *a*) to 12 % (Fig. 2, *d*).

At the end of the combustion process, the volume of the air zone is mixed with the volume of the CP zone to a homogeneous composition throughout the above-piston volume, which contributes to intense air supply during the afterburning of unburned fuel particles. The process of additional oxidation of fuel continues until the opening of the outlet window (102 CAD BTDC) (Fig. 2, *a–d*).

Using the three-zone combustion model based on the volume balance method allows determining the nature of changes and quantitative volume values of the CP, FAM and air zones simultaneously during the piston movement.

However, the configuration of the zones volumes during the charge movement should be refined by experimental methods.

The volume of the air zone decreases with increasing load and is absent at the maximum load. Therefore, in the range of increased loads (*bmep*=0.322 MPa), it is preferable to use the one-zone or two-zone combustion model.

The developed three-zone combustion model makes it possible to simultaneously determine the change in gas pressure in the cylinder (38), temperature in the CP (39), FAM (40) and air (41) zones when organizing SFAC. The air zone is located near the walls of the above-piston volume.

In the partial load modes (*bmep*=0.144 MPa (Fig. 3, *a*), *bmep*=0.144 MPa (Fig. 3, *b*), *bmep*=0.144 MPa (Fig. 3, *c*), *bmep*=0.144 MPa (Fig. 3, *d*)), using the three-zone combustion model, gas pressures in the cylinder by the crank angle were calculated. With increasing load from bmep=0.144 MPa to *bmep*=0.322 MPa, the maximum combustion pressure (p_z) increases from 3.75 MPa (8 CAD ATDC) (Fig. 3, *a*) to 44.21 MPa (13 CAD ATDC) (Fig. 3, *d*). The discrepancy between the results of modeling and experimental studies does not exceed 5 %. Therefore, the three-zone combustion model allows, with sufficient accuracy for practical purposes, calculating the operating process of the SFAC SI engine taking into account the air zone near the walls of the above-piston volume.

Formation of the air zone near the walls helps to reduce heat losses and increase the efficiency of converting fuel chemical energy during combustion into efficient operation. However, creating a uniform air layer near the walls is challenging.

In the engine operating modes (*bmep*=0.144, 0.192, 0.274, 0.322 MPa), the characteristics of temperature variation in the CP (39), FAM (40) and air (41) zones were calculated. The values of average temperatures in the cylinder were determined according to the one-zone combustion model (14) (Fig. 3).

In the minimum load mode (*bmep*=0.144 MPa), the maximum temperature value in the CP zone is $T_{CP\,\max}$=2002 K at 5 CAD BTDC (Fig. 3, *a*). During the combustion process, the temperature in the FAM volume and air zones rises. The maximum average temperature of the working fluid in the above-piston volume is T_{average}=1,849 K (11 CAD ATDC).

In the engine partial load mode (bmep=0.192 MPa), the maximum temperature of CP is $T_{CP\,\max}$=2234 *K* at 4 CAD BTDC (Fig. 3, *b*). Further course of the combustion process is accompanied by a temperature increase in the FAM volume zone and in the air zone. The maximum average temperature in the above-piston volume is $T_{average}$=2,047 *K* (14 CAD ATDC).

In the medium load modes (*bmep*=0.274 MPa and *bmep*=0.322 MPa), temperature values for the CP, FAM, air zones and average temperature in the cylinder were determined (Fig. 3, *c*). The maximum temperature of CP is 2,994 K (4 CAD BTDC) at *bmep*=0.274 MPa, and *bmep*=0.322 MPa – 3,084 K (2 CAD BTDC). The maximum average temperature in the cylinder at *bmep*=0.274 MPa – 2,427 K (17 CAD ATDC) and 2,578 K (19 CAD ATDC) at *bmep*=0.322 MPa.

Using the three-zone combustion model, which makes it possible to more accurately determine the temperature in the CP zone, relative to the average temperature over the entire above-piston volume, is undoubtedly expedient in modeling combustion products, in particular, nitrogen oxides.

The developed three-zone combustion model based on the volume balance method is the basis and can be improved and supplemented with various sub-models describing physical and chemical processes of internal mixture formation and SFAC combustion.

For example, a combustion submodel can include a combustion model taking into account the flow rate of laminar or turbulent flame, various models for calculating the concentration of complete and incomplete combustion products, nitrogen oxides. Calculations of combustion processes can also take into account the impact of alternative fuels, exhaust gas recirculation on exhaust gas toxicity.

The three-zone combustion model allows estimating the combustion rate by calculating the change in the CP zone volume relative to the FAM zone volume, however, the composition or density of the working fluid should be taken into account.

The results of calculating indicator diagrams using the three-zone combustion model can be used to determine the indicator and effective parameters of engines. However, in the high load modes, where there is no FAM stratification with the air zone, or with homogeneous composition of FAM over the entire cylinder volume, other models should be used that do not take into account the air zone.

The three-zone model can be refined by adapting the initial data based on three-dimensional modeling of operating processes in the engine cylinder. The use of experimental methods for recording physical processes, for example, high-speed filming, thermal imaging, laser, X-ray devices, etc., allows taking into account real volumes of zones, their parameters and compositions in the model.

The research results do not contradict the main provisions of fundamental works [12, 26, 28, 29, 49, 52–54]. At the same time, the results of the studies are consistent with the hypothesis of stratified FAC during the formation of a separate air zone during combustion.

7. Conclusions

1. The differential equation of the processes of internal mixture formation with DI and SFAC at the compression stroke with closed valves was compiled, including:

– adiabatic change in the SFAC volume, consisting of the FAM volume and air volume with the distribution of CP residues over the considered volumes;

– change in the volume of the working fluid in the above-piston volume due to external heat transfer;

– change in the FAM volume in the above-piston volume due to physical processes during liquid fuel evaporation;

– change of the above-piston volume during the piston movement;

– change in the above-piston volume during leaks of the working fluid through the clearance between the piston rings and cylinder walls.

Based on the obtained heat balance equation, the change in heat amount due to heat transfer between the working fluid and the adjacent walls of the above-piston volume is taken into account. The equation takes into account the heat involved in gasoline evaporation in the fuel stream and from the surface of the fuel film.

2. Basic equations of the SFAC combustion-expansion processes were derived on the basis of the three-zone model, taking into account the volumes in the corresponding CP, FAM and air zones, as well as their ratios. At the same time, the differential equation of the volume balance of combustion-expansion processes was created taking into account three zones in the corresponding CP (V_{CP}), FAM (V_{FAM}) and air (V_{air}) volumes, as well as their ratios. The equation takes into account the change in the volume of the working fluid due to heat transfer and heat exchange between the zones and the walls of the above-piston volume. On the basis of the obtained heat balance equations, changes in heat fluxes for the CP, FAM and air zones were determined due to heat transfer and heat exchange between the zones and the walls of the above-piston volume.

3. Dependences for the simultaneous determination of the working fluid temperature in the V_{CP}, V_{FAM} and V_{air} volume zones are presented taking into account heat transfer between the zones and the adjoining walls. Pressure in the above-piston volume is determined by the dependence considering the corresponding three zones during combustion.

4. Based on the calculation results, graphs of volume changes of the FAM, CP and air zones with the change in the above-piston volume and organizing stratified lean FAC in partial load modes at n=3,000 rpm were plotted. With increasing load from $bmep$=0.144 MPa to $bmep$=0.322 MPa, at the moment of ignition, the volume of the FAM zone increases from 70 % to 92 % of the above-piston volume. In this case, the volume of the air zone decreases from 30 % to 8 %.

5. Comparative analysis of theoretical and experimental indicator diagrams in the load characteristic modes (n= =3000 rpm) of the 1D 8.7/8.2 two-stroke DI SI engine was carried out. The research analysis showed that when adjusting the heat transfer formula and the constant C_2, taking into account the peculiarities of the operating process with the SFAC, discrepancies in the maximum combustion pressure do not exceed 5 %. The level and nature of temperature changes in the volumes of the CP, FAM and air zones, determined by the three-zone model, are consistent with the theory of ICE operating processes. The use of the developed three-zone model for calculating the operating process of the DI SI engine will reduce the time and costs for conducting experimental studies on the refinement of the operating processes with SFAC.

References

1. World Energy Outlook 2020. IEA. Available at: https://www.iea.org/reports/world-energy-outlook-2020
2. Parsadanov, I., Marchenko, A., Tkachuk, M., Kravchenko, S., Polyvianchuk, A., Strokov, A. et. al. (2020). Complex Assessment of Fuel Efficiency and Diesel Exhaust Toxicity. SAE Technical Paper Series. doi: https://doi.org/10.4271/2020-01-2182
3. Liu, W. (2013). Introduction to Hybrid Vehicle System Modeling and Control. John Wiley & Sons Ltd. doi: https://doi.org/10.1002/9781118407400
4. Migal, V., Lebedev, A., Shuliak, M., Kalinin, E., Arhun, S., Korohodskyi, V. (2020). Reducing the vibration of bearing units of electric vehicle asynchronous traction motors. Journal of Vibration and Control, 107754632093763. doi: https://doi.org/10.1177/1077546320937634
5. Leontiev, D. N., Voronkov, O., Korohodskyi, V., Hlushkova, D., Nikitchenko, I., Teslenko, E., Lykhodii, O. (2020). Mathematical Modelling of Operating Processes in the Pneumatic Engine of the Car. SAE Technical Paper Series. doi: https://doi.org/10.4271/2020-01-2222
6. Panchuk, M., Kryshtopa, S., Sladkowski, A., Kryshtopa, L., Klochko, N. et. al. (2019). Effi ciency of Production of Motor Biofuels for Water and Land Transport. Naše More, 66 (3), 6–12. doi: https://doi.org/10.17818/nm/2019/3.8
7. Kryshtopa, S., Kryshtopa, L., Panchuk, M., Smigins, R., Dolishnii, B. (2021). Composition and energy value research of pyrolise gases. IOP Conference Series: Earth and Environmental Science, 628, 012008. doi: https://doi.org/10.1088/1755-1315/628/1/012008
8. Kryshtopa, S., Kryshtopa, L., Melnyk, V., Dolishnii, B., Prunko, I., Demianchuk, Y. (2017). Experimental research on diesel engine working on a mixture of diesel fuel and fusel oils. Transport Problems, 12 (2), 53–63. doi: https://doi.org/10.20858/tp.2017.12.2.6
9. Panchuk, M., Kryshtopa, S., Panchuk, A. (2020). Innovative Technologies for the Creation of a New Sustainable, Environmentally Neutral Energy Production in Ukraine. 2020 International Conference on Decision Aid Sciences and Application (DASA). doi: https://doi.org/10.1109/dasa51403.2020.9317165
10. Panchuk, M., Kryshtopa, S., Panchuk, A., Kryshtopa, L., Dolishnii, B., Mandryk, I., Sladkowski, A. (2019). Perspectives for developing and using the torrefaction technology in Ukraine. International Journal of Energy for a Clean Environment, 20 (2), 113–134. doi: https://doi.org/10.1615/interjenercleanenv.2019026643
11. Panchuk, M., Kryshtopa, S., Sładkowski, A., Panchuk, A. (2020). Environmental Aspects of the Production and Use of Biofuels in Transport. Lecture Notes in Networks and Systems, 115–168. doi: https://doi.org/10.1007/978-3-030-42323-0_3
12. Van Basshuysen, R. (Ed.) (2017). Ottomotor mit Direkteinspritzung und Direkteinblasung. Springer, 621. doi: https://doi.org/10.1007/978-3-658-12215-7
13. Alturki, E. W. (2017). Four-Stroke and Two-Stroke Marine Engines Comparison and Application. International Journal of Engineering Research and Applications, 07 (04), 49–56. doi: https://doi.org/10.9790/9622-0704034956
14. Eroschenko, S. A., Korogodskiy, V. A., Kagramanyan, A. A., Vrublevskiy, A. N., Vasilenko, O. V., Oboznyy, S. V. (2012). Eksperimental'nye issledovaniya dvigatelya s iskrovym zazhiganiem i neposredstvennym vpryskivaniem topliva pri rabote na benzo-etanol'noy

smesi. Dvigateli vnutrennego sgoraniya, 1, 8–9. Available at: http://repository.kpi.kharkov.ua/bitstream/KhPI-Press/61/1/DVS_2012_1_Eroshenkov_Eksperimentalnye%20issledovaniya.pdf
15. Korohodskyi, V. (2020). Comparison of technical, economic and environmental indicators of two-stroke and fourstroke engines according to load characteristics. Bulletin of Kharkov National Automobile and Highway University, 90, 80–94. doi: https://doi.org/10.30977/bul.2219-5548.2020.90.0.80
16. Korohodskyi, V., Khandrymailov, A., Stetsenko, O. (2016). Dependence of the coefficients of residual gases on the type of mixture formation and the shape of a combustion chamber. Eastern-European Journal of Enterprise Technologies, 1 (5 (79)), 4–12. doi: https://doi.org/10.15587/1729-4061.2016.59789
17. Korohodskyi, V., Voronkov, A., Migal, V., Nikitchenko, I., Zenkin, E., Rublov, V., Rudenko, N. (2020). Determining the criteria and the degree of the stratification of the air-fuel charge in a cylinder of a spark-ignition engine during injecting fuel. IOP Conference Series: Materials Science and Engineering, 977, 012002. doi: https://doi.org/10.1088/1757-899x/977/1/012002
18. Korohodskyi, V., Kryshtopa, S., Migal, V., Rogovyi, A., Polivyanchuk, A., Slyn'ko, G. et. al. (2020). Determining the characteristics for the rational adjusting of an fuel-air mixture composition in a two-stroke engine with internal carburation. Eastern-European Journal of Enterprise Technologies, 2 (5 (104)), 39–52. doi: https://doi.org/10.15587/1729-4061.2020.200766
19. Caton, J. (2018). The Thermodynamics of Internal Combustion Engines: Examples of Insights. Inventions, 3 (2), 33. doi: https://doi.org/10.3390/inventions3020033
20. Bajwa, A. U., Patterson, M., Linker, T., Jacobs, T. J. (2019). A New Single-Zone Multi-Stage Scavenging Model for Real-Time Emissions Control in Two-Stroke Engines. ASME 2019 Internal Combustion Engine Division Fall Technical Conference. doi: https://doi.org/10.1115/icef2019-7198
21. De Faria, M. M. N., Vargas Machuca Bueno, J. P., Ayad, S. M. M. E., Belchior, C. R. P. (2017). Thermodynamic simulation model for predicting the performance of spark ignition engines using biogas as fuel. Energy Conversion and Management, 149, 1096–1108. doi: https://doi.org/10.1016/j.enconman.2017.06.045
22. Finesso, R., Spessa, E. (2014). A real time zero-dimensional diagnostic model for the calculation of in-cylinder temperatures, HRR and nitrogen oxides in diesel engines. Energy Conversion and Management, 79, 498–510. doi: https://doi.org/10.1016/j.enconman.2013.12.045
23. Douvartzides, S., Karmalis, I., Ntinas, N. (2020). Thermodynamic Cycle Analysis of an Automotive Internal Combustion Engine With the Characteristics of the Commercial BMW N54 Spark-Ignition Model. Journal of Energy Resources Technology, 142 (10). doi: https://doi.org/10.1115/1.4046600
24. Caton, J. A. (2018). Maximum efficiencies for internal combustion engines: Thermodynamic limitations. International Journal of Engine Research, 19(10), 1005–1023. doi: https://doi.org/10.1177/1468087417737700
25. Wissink, M. L., Splitter, D. A., Dempsey, A. B., Curran, S. J., Kaul, B. C., Szybist, J. P. (2017). An assessment of thermodynamic merits for current and potential future engine operating strategies. International Journal of Engine Research, 18 (1-2), 155–169. doi: https://doi.org/10.1177/1468087416686698
26. Merker, G. P., Teichmann, R. (Eds.) (2014). Grundlagen Verbrennungsmotoren. Funktionsweise, Simulation, Messtechnik. Springer, 1132. doi: https://doi.org/10.1007/978-3-658-03195-4
27. Kavtaradze, R. Z., Onischenko, D. O. (2013). Modelirovanie i raschet rabochego protsessa v dvigatelyah. Odnozonnye i mnogozonnye modele. V kn. RAN. Mashinostroenie. Entsiklopediya. Vol. IV-14. Dvigateli vnutrennego sgoraniya. Moscow: Mashinostroenie, 102–113. Available at: https://ua1lib.org/book/3240340/497a21?regionChanged=&redirect=227103051
28. Pischinger, R., Klell, M., Sams, T. (2009). Thermodynamik der Verbrennungskraftmaschine. Springer, 475. doi: https://doi.org/10.1007/978-3-211-99277-7
29. Medina, A., Curto-Risso, P. L., Hernández, A. C., Guzmán-Vargas, L., Angulo-Brown, F., Sen, A. K. (2014). Quasi-Dimensional Simulation of Spark Ignition Engines. Springer-Verlag, 195. doi: https://doi.org/10.1007/978-1-4471-5289-7
30. Wang, Y. (2020). A Novel Two-Zone Thermodynamic Model for Spark-Ignition Engines Based on an Idealized Thermodynamic Process. Energies, 13 (15), 3801. doi: https://doi.org/10.3390/en13153801
31. Stepanenko, D., Kneba, Z. (2019). Thermodynamic modeling of combustion process of the internal combustion engines – an overview. Combustion Engines, 178 (3), 27–37. doi: https://doi.org/10.19206/ce-2019-306
32. Kaprielian, L., Demoulin, M., Cinnella, P., Daru, V. (2013). Multi-Zone Quasi-Dimensional Combustion Models for Spark-Ignition Engines. SAE Technical Paper Series. doi: https://doi.org/10.4271/2013-24-0025
33. Baratta, M., Ferrari, A., Zhang, Q. (2018). Multi-zone thermodynamic modeling of combustion and emission formation in CNG engines using detailed chemical kinetics. Fuel, 231, 396–403. doi: https://doi.org/10.1016/j.fuel.2018.05.088
34. Monteiro, E., Rouboa, A., Bellenoue, M., Boust, B., Sotton, J. (2014). Multi-zone modeling and simulation of syngas combustion under laminar conditions. Applied Energy, 114, 724–734. doi: https://doi.org/10.1016/j.apenergy.2012.08.027
35. Sun, Z. Y., Xu, C. (2020). Turbulent burning velocity of stoichiometric syngas flames with different hydrogen volumetric fractions upon constant-volume method with multi-zone model. International Journal of Hydrogen Energy, 45 (7), 4969–4978. doi: https://doi.org/10.1016/j.ijhydene.2019.12.054
36. Azarmanesh, S., Targhi, M. Z. (2021). Comparison of laser ignition and spark plug by thermodynamic simulation of multi-zone combustion for lean methane-air mixtures in the internal combustion engine. Energy, 216, 119309. doi: https://doi.org/10.1016/j.energy.2020.119309

37. Bhat, V., Tamma, B. (2014). Development of Multi-Zone Phenomenological Model for SI Engine. SAE Technical Paper Series. doi: https://doi.org/10.4271/2014-01-1068
38. Glagolev, N. M. (1950). Rabochie protsessy dvigateley vnutrennego sgoraniya. Moscow: Mashgiz, 480. Available at: https://ua1lib.org/book/2445345/fa8d8f
39. D'yachenko, V. G. (1970). Differentsial'nye uravneniya protsessa gazoobmena dvigateley vnutrennego sgoraniya. Dvigateli vnutrennego sgoraniya, 11, 17–24. Available at: https://www.twirpx.com/file/935076/
40. Martyr, A. J., Plint, M. A. (2012). Engine Testing. The Design, Building, Modification and Use of Powertrain Test Facilities. Butterworth-Heinemann. doi: https://doi.org/10.1016/c2010-0-66322-x
41. Bernhard, F. (Ed.) (2014). Handbuch der Technischen Temperaturmessung. Springer Vieweg, 1619. doi: https://doi.org/10.1007/978-3-642-24506-0
42. Korogodskiy, V. A., Stetsenko, O. N. (2016). Rezul'taty modelirovaniya protsessa sgoraniya rassloennogo toplivno-vozdushnogo zaryada v dvuhtaktnom dvigatele s iskrovym zazhiganiem. Mizhnar. nauk.-prakt. ta nauk.-metod. konf.: Novitni tekhnolohiyi v avtomobilebuduvanni, transporti i pry pidhotovtsi fakhivtsiv. Kharkiv: KhNADU, 216–217. Available at: https://af.khadi.kharkov.ua/fileadmin/F-AUTOMOBILE/%D0%9A%D0%BE%D0%BD%D1%84%D0%B5%D1%80%D0%B5%D0%BD%D1%86%D1%96%D1%97/2016_conf_III/sbornik_2016.pdf
43. Kulygin, V. I., Korogodskyj, V. A., Kyrylyuk, I. O., Lomov, S. G. (2007). Pat. No. WO/2009/044225. A Method of Mixing in a Combustion Chamber of an Internal Combustion Engine and a Spark-Ignition Direct-Injection Stratified Fuel-Air Charge Internal Combustion Engine. No. WO/2009/044225; declareted: 27.12.2007; published: 09.04.2009. Available at: https://patentscope.wipo.int/search/en/detail.jsf?docId=WO2009044225&tab=PCTBIBLIO
44. Hoppe, N., Weberbauer, F., Woschni, G., Zeilinger, K. (2003). Experimentelle Erfassung und Simulation des Betriebsverhaltens von Ottomotoren mit Direkteinspritzung. MTZ – Motortechnische Zeitschrift, 64 (7-8), 628–635. doi: https://doi.org/10.1007/bf03227117
45. Korogodskiy, V. A. (2017). Nauchnye osnovy perspektivnyh rabochih protsessov dvigateley s vnutrennim smeseobrazovaniem i iskrovym zazhiganiem. Kharkiv: KhNADU, 380. Available at: http://library.kpi.kharkov.ua/uk/technics_Naospd
46. Korohodskiy, V. A., Stetsenko, O. N., Tkachenko, E. A. (2015). The influence stratification of fuel and air charge on combustion indicators two-stroke engines with spark ignition. Collection of scientific works of the Ukrainian State University of Railway Transport, 154, 142–148. doi: https://doi.org/10.18664/1994-7852.154.2015.66009
47. Petrichenko, R. M. (1983). Fizicheskie osnovy vnutritsilindrovyh protsessov v dvigatelyah vnutrennego sgoraniya. Leningrad: LGU, 244. Available at: https://ua1lib.org/book/3084734/bb9887?regionChanged=&redirect=227115960
48. Spektorov, L. G., Gurlyand, A. D. (1975). Raschet ispareniya benzina s poverhnosti zhidkoy plenki pri vpryske v dvigatel' s vosplameneniem ot iskry. Dvigateli vnutrennego sgoraniya, 22, 103–110. Available at: https://www.twirpx.com/file/1564689/
49. D'yachenko, V. G. (2009). Teoriya dvigateley vnutrennego sgoraniya. Kharkiv: KhNADU, 500. Available at: https://1lib.nl/book/1275641/e44835
50. Vibe, I. I. (1962). Novoe o rabochem tsikle dvigateley. Moscow: Mashgiz, 272. Available at: https://ua1lib.org/book/2445326/eafc04
51. Kavtaradze, R. Z. (2016). Lokal'niy teploobmen v porshnevyh dvigatelyah. Moscow: Izd-vo MGTU im. N.E. Baumana, 520.
52. Kavtaradze, R. Z. (2016). Teoriya porshnevyh dvigateley. Spetsial'nye glavy. Moscow: MGTU im. N.E. Baumana, 589. Available at: https://ua1lib.org/book/4988543/f696f3
53. Caton, J. A. (Ed.) (2015). An Introduction to Thermodynamic Cycle Simulations for Internal Combustion Engines. John Wiley & Sons, Ltd, 367. doi: https://doi.org/10.1002/9781119037576
54. Heywood, J. B. (2018). Internal Combustion Engine Fundamentals. McGraw-Hill Education. Available at: https://www.accessengineeringlibrary.com/content/book/9781260116106